



Published in final edited form as:

Cancer Res. 2013 September 1; 73(17): 5416–5425. doi:10.1158/0008-5472.CAN-13-0362.

FOXL1, a Novel Candidate Tumor Suppressor, Inhibits Tumor Aggressiveness and Predicts Outcome in Human Pancreatic Cancer

Geng Zhang¹, Peijun He¹, Jochen Gaedcke², B. Michael Ghadimi², Thomas Ried³, Harris G. Yfantis⁴, Dong H. Lee⁴, Nader Hanna⁵, H. Richard Alexander⁵, and S. Perwez Hussain¹

¹Pancreatic Cancer Unit, Laboratory of Human Carcinogenesis, Center for Cancer Research, National Cancer Institute, National Institutes of Health, Bethesda, MD, USA

²Department of General and Visceral Surgery, University Medicine, Göttingen, Germany

³Genetics Branch, National Cancer Institute, NIH, Bethesda, MD, USA

⁴Pathology and Laboratory Medicine, Baltimore Veterans Affairs Medical Center, Baltimore, MD, USA

⁵Division of Surgical Oncology, The Department of Surgery and the Marlene and Stewart Greenebaum Cancer Center, University of Maryland School of Medicine, Baltimore, MD, USA

Abstract

The Forkhead Box L1 (FOXL1) transcription factor regulates epithelial proliferation and development of gastrointestinal tract, and has been implicated in gastrointestinal tumorigenesis in mouse models. However, the role of FOXL1 in pancreatic cancer development and progression remains to be elucidated. Here, we report that a higher expression of FOXL1 is significantly associated with better clinical outcome in human pancreatic ductal adenocarcinoma (PDAC). A lower FOXL1 expression is correlated with metastasis and advanced pathological stage of pancreatic cancer. Mechanistic analyses demonstrated that over-expression of FOXL1 induces apoptosis and inhibits proliferation and invasion in pancreatic cancer cells, whereas silencing of FOXL1 by siRNA inhibits apoptosis and enhances tumor cell growth and invasion. Furthermore, FOXL1 overexpression significantly suppressed the growth of tumor xenografts in nude mice. FOXL1 promoted apoptosis partly through the induction of TNF-related apoptosis-inducing ligand (TRAIL) in pancreatic cancer cells. In addition, FOXL1 suppressed the transcription of zinc finger E-box-binding homeobox 1 (ZEB1), an activator of epithelial mesenchymal transition (EMT), and the negative regulation of ZEB1 contributed to the inhibitory effect of FOXL1 on tumor cell invasion. Taken together, our findings suggest that FOXL1 expression is a candidate predictor of clinical outcome in patients with resected PDAC and it plays an inhibitory role in pancreatic tumor progression.

Keywords

FOXL1; pancreatic cancer; prognosis; TRAIL; ZEB1

Corresponding Author: S. Perwez Hussain, Pancreatic Cancer Unit, Laboratory of Human Carcinogenesis, National Cancer Institute, National Institutes of Health, 37 Convent Drive, Building 37, Room 3044B, Bethesda, MD 20892. Phone: (301) 402-3431; Fax: (301) 496-0497; hussainp@mail.nih.gov.

The authors disclose no potential conflicts of interest.

Introduction

Pancreatic cancer is the fourth leading cause of cancer death in the United States (1). The median survival of all PDAC cases is less than 6 months, and only 6% of patients survive 5 years after diagnosis. The dismal prognosis in pancreatic cancer is due to late diagnosis and the lack of effective treatment. A better understanding of the molecular mechanism of this disease and discovery of novel therapeutic targets are desperately needed to improve outcomes in patients with PDAC.

FOXL1 proteins belong to the forkhead box (Fox) family of transcription factors. Fox family shares a highly conserved 100-aa DNA binding domain (the forkhead box) and comprises more than 100 members in humans, classified as FOXA to FOXR on the basis of sequence similarity (2). Fox proteins are at the junction of multiple signaling pathways and play critical roles in a variety of physiological and pathological processes including cancer. For example, FOXOs can initiate apoptosis and promote cell cycle arrest (3). In addition, FOXOs deficiency in genetic mice led to the development of thymic lymphomas and haemangiomas, indicating that the FOXOs are tumor suppressors (4, 5). In contrast to FOXOs, FOXM1 has been shown to have pro-proliferative function and increased expression of FOXM1 gene was often found in various human cancers (6). In pancreatic cancer, overexpression of FOXM1 is associated with poor prognosis and pathologic stage of pancreatic ductal adenocarcinoma (7). Down-regulation of FOXM1 results in the inhibition of migration, invasion, and angiogenesis of PDAC (8).

FOXL1 has been implicated in the regulation of epithelial cell proliferation in gastrointestinal tracts. Loss of *Foxl1* led to a marked increase in cellular proliferation of intestinal epithelia in mice, leading to the distortion in the tissue architecture of the stomach and small intestine (9). The altered proliferation rate in *Foxl1*-null mutant mice is correlated with an activated Wnt/ β -catenin pathway as demonstrated by increased nuclear translocation of β -catenin (10). *Foxl1* deficiency accelerates the initiation of gastrointestinal tumor and increases tumor load in *Apc^{Min}* mice (11). FOXL1 is specifically expressed in low-grade fibromyxoid sarcoma (LGFMS), as compared to other morphologically similar tumor types including myxofibrosarcoma, desmoid fibromatosis, extraskeletal myxoid chondrosarcoma and solitary fibrous tumors, suggesting its role in LGFMS (12). Thus far, the biological function of FOXL1 in human cancer remains to be elucidated. In the present study, we investigated the role of FOXL1 in human pancreatic cancer. Our data demonstrated that FOXL1 expression is associated with clinical outcomes, pathological stages and metastasis of pancreatic cancer. Further mechanistic studies showed that FOXL1 inhibits cellular proliferation and invasion in pancreatic cancer cells. Moreover, we investigated the potential transcriptional targets of FOXL1, which may contribute to the inhibitory effects of FOXL1 on the growth and invasion in human pancreatic cancer cells.

Materials and Methods

Tissue Collection and RNA Isolation

Pairs of primary pancreatic tumor and adjacent non-tumor tissues came from 45 patients with PDAC at the Department of General and Visceral Surgery, University Medicine Göttingen, Göttingen, Germany. Tissues were flash frozen immediately after surgery. Demographic and clinical information for each case included age, sex, grade, clinical staging, resection margin status, and survival times from diagnosis (Table S1). Tumor histopathology was classified according to the World Health Organization Classification of Tumor system (13). Use of these clinical specimens was reviewed and permitted by the NCI-Office of the Human Subject Research (OHSR, Exempt # 4678) at the National Institutes of Health, Bethesda, MD. RNA from frozen tissue samples was extracted using

standard TRIZOL (Invitrogen, Carlsbad, CA) protocol. RNA quality was confirmed with the Agilent 2100 Bioanalyzer (Agilent Technologies).

Quantitative RT-PCR (qRT-PCR)

Total RNA was reverse transcribed using High-Capacity cDNA Reverse Transcription Kit (Applied Biosystems, Foster City, CA). qRT-PCR reactions in 384 well plates were performed using Taqman Gene Expression Assays on an ABI Prism 7900HT Sequence Detection instrument from Applied Biosystems. Expression levels of ACTB and GAPDH were used as the endogenous controls. All assays were performed at least in triplicates. For quality control, any samples with a gene cycle value greater than 36 were considered of poor quality and removed. If a tumor or non-tumor sample failed quality control from qRT-PCR that case was removed from the analysis. All the primers for qRT-PCR in the present study were purchased from Applied Biosystems.

Immunohistochemistry (IHC)

5 μ m thick paraffin sections of tumors and surrounding non-tumor tissues from resected PDAC cases were incubated with mouse monoclonal anti-FOXL1 antibody (Abnova, Walnut, CA). Signals were amplified using biotinylated IgG, followed by horseradish peroxidase-conjugated avidin-biotin complex (Vectastain ABC Kit, Vector Lab, Burlingame, CA) and diaminobenzene (DAB) as the chromogen (Dako Envision System, Carpinter, CA). Immunostaining was evaluated blindly by two Board-certified pathologist assigning the intensity and prevalence score as described elsewhere (14). Briefly, the intensity was assigned a score of 0–3, representing negative, weak, moderate or strong expression, whereas, prevalence was assigned a score of 0–4 representing <10%, 10–30%, 30–50%, 50–80% and >80% cells showing FOXL1 expression. The overall quantitation of IHC score was then achieved by multiplying the intensity and prevalence score as described elsewhere (15). IHC images were photographed under an Olympus BX40 microscope.

Cell lines and culture conditions

Human pancreatic carcinoma cell lines Panc1 (CRL-1469TM), MIApaca2 (CRL-1420TM) and Capan-1 (HTB-79TM), were obtained from American Type Culture Collection ATCC (Rockville, MD, USA). Cells were maintained in GIBCO RPMI Media 1640 supplemented with GlutaMAXTM-I (Invitrogen), penicillin-streptomycin (50 IU/ml and 50 mg/ml, respectively), and 10% (v/v) fetal calf serum (FCS). Cells were incubated at 37°C in a humidified atmosphere with 10% CO₂. Transfection of the plasmid was performed using Lipofectamine LTX reagent according to the manufacturer's protocol (Invitrogen). Plasmid pCMV-CTRL was used for transfection as the negative control. Plasmid pCMV-FOXL1 was used for FOXL1 overexpression. ON-TARGET^{plus} siRNAs targeting to FOXL1 or ZEB1 and DharmaFECT-4 (Dharmacon, Lafayette, CO) were used for silencing FOXL1 or ZEB1 expression in pancreatic cancer cells.

MTT assay

Cells were seeded in 96-well plates (3,000 cells/well) and incubated for 2–10 days. Then, the MTT solution was added and incubated for 4 hours. After the MTT solution was aspirated, 100ul dimethylsulfoxide (DMSO) was added to each well. The absorbance was measured at 570nm and 650 nm.

Apoptosis assay

Pancreatic cancer cell lines were seeded and transfected with FOXL1 over-expression vectors or siRNAs directly targeting FOXL1 mRNA. Caspase activity was measured by

Apo-ONE™ Homogeneous Caspase-3/7 Assay (Promega, Madison, WI) and potency of caspase activation was calculated compared to control cells.

Quantification of TRAIL protein level by ELISA

Cells were transfected with either control vector pCMV-CTRL or pCMV-FOXL1 expression vectors respectively. 24h following transfection, cells were sorted and aliquoted in sample tubes (5×10^5 cells/ sample). Cells were lysed (5×10^5 cells/ 100ul lysate buffer) and TRAIL production in cell lysates was measured using Quantikine Human TRAIL/ TNFSF10 ELISA KIT (R&D Systems, Minneapolis, MN) according to the manufacturer's instructions. Optical density of each well was then determined using a microplate reader set to 450 nm. TRAIL concentrations were calculated using a standard curve and linear regression analysis.

Subcutaneous xenografts in nude mice

All animal experiments and maintenance conformed to the guidelines of the Animal Care and Use Committee and of the American Association of Laboratory Animal Care. 5×10^6 FOXL1-overexpressing cells and control Panc1 cells in a total volume of 100 μ L of 1/1 (v/v) PBS/matrigel (BD Biosciences: Sparks, MD) were injected subcutaneously into flanks of 8–9 weeks old male athymic nu/nu mice (Harlan Laboratories, Indianapolis, IN) with 5 mice per arm. One week after the injection of tumor cells, subcutaneous tumor volumes (V) were measured weekly with digital calipers (Fisher Scientific: Pittsburgh, PA) and calculated using the formula $V = 1/2(ab^2)$, where a is the biggest and b is the smallest orthogonal tumor diameter. After 6 weeks, all mice were sacrificed and xenografts were resected and measured. Differences in tumor growth were compared by the two-way repeated measures ANOVA, and comparisons of tumor weight between the groups were made using the two-tailed Student's t-test. A p-value of <0.05 is considered significant.

Cell invasion assay

Pancreatic cancer cell invasion assay was performed in 24-well Biocoat Matrigel invasion chambers (8 μ m; Becton Dickinson, Franklin Lakes, NJ) according to the manufacturer's protocol. Briefly, cells were transfected with either control vector pCMV-GFP or pCMV-FOXL1-GFP expression vectors respectively. 24h following transfection, cells were harvested and plated in the top chamber (5×10^4 /well). The bottom chamber contained 10% FBS as a chemoattractant. After 48h incubation, the noninvasive cells were removed with a cotton swab. The invasive cells migrate through the membrane and stick to the lower surface of the membrane. GFP-positive cells were counted under a fluorescence microscope in five fields (20X magnification). Data are expressed as the percent invasion according to the manufacturer's manual: the number of the cells invading through the Matrigel membrane divided by the number of cells migrating through the control membrane. All assays were performed in triplicate and repeated three times.

Luciferase assay

Human ZEB1 or TRAIL promoter fragment was amplified from genomic DNA by PCR and cloned into pGL4Basic vector (Promega). Briefly, 1 μ g pCMV-FOXL1 (or pCMV-CTRL), and 1 μ g of firefly-luciferase reporter plasmid (pGL4-ZEB or pGL4-TRAIL) together with 10ng of a Renilla luciferase transfection control (pRL-TK; Promega) were incubated overnight with sub-confluent cell cultures in each well of a 24-well plate. The cells were then washed twice in PBS and harvested for firefly/Renilla luciferase assays using the Dual-Luciferase Reporter Assay System (Promega).

Chromatin immunoprecipitation (ChIP) assays

Chromatin immunoprecipitation (ChIP) assays were performed according to the manufacturer's instructions (Qiagen, Valencia, CA). Briefly, Panc1 cells were transfected with pCMV-FOXL1-GFP. Forty-eight hours following transfection, formaldehyde was added to cell culture media to a final concentration of 1% and then the cells were incubated for 10 minutes on a shaking platform at RT. After the addition of glycine at concentrations of up to 0.136M, cells were incubated for 5 minutes and then washed with cold PBS. Cell pellets were obtained, resuspended in sodium dodecyl sulfate lysis buffer, and sonicated with a Bioruptor (Cosmo Bio, Carlsbad, CA) for 30 seconds at maximum setting 10 times at 1-minute intervals. Immunoprecipitation was carried out overnight at 4°C with rotation, using antibodies specific for GFP (Origene, Rockville, MD) or mouse control IgG. After incubation with protein A, the beads were collected, washed, and eluted per manufacturer's instructions. Cross-links were reversed by incubation for 6 hours at 65°C, and DNA was purified from the supernatant by phenol/chloroform extraction and ethanol precipitation. Precipitated DNA was analyzed by qRT-PCR. The PCR primer pairs spanned upstream of promoter region of the human *ZEB1* gene (GenBank accession number NM_001128128): (1) forward, 5'-TTCGAAGGGCTGGCATGGGT-3'; reverse, 5'-CACCGTGGAAACAAAGGAGGGCA-3'; (2) forward, 5'-GCAGGGAGGTACAGGCCAGA-3'; reverse, 5'-TTGACCCACCCAC CAACA-3'; (3) forward, 5'-TGACCGCGTCCCTACGGTTT-3'; reverse, 5'-ACGGCCGGA ACCTTGTGCT-3'; (4) forward, 5'-TTGTGCTGTGTG CCAAGGGAA-3'; reverse, 5'-AAAGGCGACTGTGCAACCACCA-3'. The PCR primer pairs spanned upstream of promoter region of the human *TNFSF10* gene (TRAIL, GenBank accession number NM_003810.2): forward, 5'-TGCATGGATCCTGA GGGCAAGG -3'; reverse, 5'-TTGAACCTGCAACTGTCCCTCCC-3'. Quantitative RT-PCR conditions were used: 35 cycles of 94°C for 45 seconds; 60°C for 45 seconds; and 72°C for 45 seconds.

Statistical Analysis

Expression graphs and student *t*-test were used to analyze differences in gene expression using Graphpad Prism 5.0 (Graphpad Software Inc, San Diego, California). Kaplan-Meier analysis was performed with Graphpad Prism 5.0. Cox Proportional-hazards regression analysis was performed using Stata 11 (StataCorp LP, College Station, Texas). Univariate Cox regression was performed on genes and clinical covariates to examine influence of each on patient survival. Final multivariate models were based on stepwise addition and removal of clinical covariates found to be associated with survival in univariate models ($P < 0.05$). For these models, resection margin status was dichotomized as positive (R1) vs negative (R0); TNM staging was dichotomized as I-II vs III-IV. All stepwise addition models gave the same final models as stepwise removal models. All univariate and multivariate Cox regression models were tested for proportional hazards assumptions based on Schoenfeld residuals, and no model violated these assumptions. The statistical significance was defined as $P < 0.05$. All *P* values reported were 2- sided.

Results

Higher FOXL1 is associated with better clinical outcome in pancreatic cancer

We performed qRT-PCR for FOXL1 in 45 tumor samples of PDAC and analyzed its association with disease outcome. We dichotomized high and low expression of FOXL1 as values above and below the median respectively, and found that a higher level of FOXL1 gene expression was associated with better survival ($P = 0.031$, Kaplan-Meier log-rank test, Figure 1A).

Univariate Cox regression analysis in PDAC cases showed that a higher FOXL1 expression (hazard ratio (HR), 0.44; 95% CI, 0.20–0.95; $P=0.036$), and differentiation grade (HR, 2.77; 95% CI, 1.12–6.87; $P=0.027$) were each associated with prognosis but not the tumor stage or resection margin status (Table 1). Multivariate analyses revealed that higher FOXL1 expression was an independent predictor of better survival (HR, 0.41; 95% CI, 0.19–0.89; $P=0.024$). Additionally, the multivariate model including FOXL1 and grade was significantly better at predicting prognosis in PDAC than grade alone ($P<0.05$, likelihood ratio test), indicating the prognostic significance of FOXL1 in resected PDAC.

IHC analysis of tumors and adjacent nontumor tissues from PDAC cases showed predominant nuclear localization of FOXL1 in pancreatic ductal cells and acinar cells (Figure 1B). PDAC cases with higher FOXL1 mRNA level determined by qRT-PCR also showed higher IHC staining score (Student's t -test $P<0.05$). FOXL1 expression was significantly higher in earlier stage (I+II) as compared with the late stage tumors (III+IV) (Student's t -test, $P<0.01$, Figure 1C). Fisher's exact test showed that a lower expression of FOXL1 is significantly correlated with PDAC cases with lymph node and distant metastases ($P<0.01$, Figure 1D). These data indicated that FOXL1 may be involved in tumor progression and aggressiveness of pancreatic cancer.

FOXL1 suppresses tumor growth of pancreatic cancer

The association of lower FOXL1 expression with increased cancer specific mortality suggests its potential inhibitory role in pancreatic tumor progression. To test this hypothesis, we first assessed the effect of FOXL1 on the proliferation and growth of pancreatic cancer cells. Panc1 and MIApaca2 pancreatic cancer cells with a lower level of endogenous FOXL1 expression (supplementary Figure S1) were transfected with pCMV-FOXL1 expression construct. An elevated expression of FOXL1 was demonstrated using qRT-PCR and western blot in cells transfected with pCMV-FOXL1, as compared with control cells (Figure 2A). Overexpression of FOXL1 significantly inhibited cell proliferation in both Panc1 and MIApaca2 cells ($P<0.05$, Figure 2B). The colony formation assay confirmed the inhibitory effect of FOXL1 on cell growth, showing a significant decrease in colony number of FOXL1-overexpressing cells compared to control cells ($P<0.01$, Figure 2C). In contrast, knock-down of FOXL1 in pancreatic cancer cells using siRNA significantly increased cell growth ($P<0.05$, supplementary Figure S3C).

To further investigate the role of FOXL1 in tumor growth of pancreatic cancer *in vivo*, we extended our investigation by subcutaneous implantation of FOXL1 overexpressing and control Panc1 cells in nude mice. Tumor growth was significantly suppressed in cells overexpressing FOXL1 as compared to control cells ($p<0.05$, Figure 2D). Overexpression of FOXL1 led to a significant reduction in tumor volume ($p<0.05$) and tumor weight ($p<0.01$) (Figure 2D). These *in vivo* findings showed that FOXL1 suppresses the tumor growth of pancreatic cancer cells.

FOXL1 increases TRAIL expression and promotes apoptosis

To determine the role of FOXL1 in regulating apoptosis in pancreatic cancer cells, we examined the caspase-3 activity in FOXL1-overexpressing Panc1 and MIApaca2 cells. Over-expression of FOXL1 led to a significant increase in caspase-3/7 activity in Panc1 and MIApaca2 cells ($P<0.01$, Figure 3A), whereas silencing of FOXL1 by siRNA reduced apoptosis as determined by caspase-3/7 activity ($P<0.01$, supplementary Figure S3D). To elucidate the underlying mechanism of the regulation of apoptosis by FOXL1, we then analyzed expressions of a panel of apoptosis related genes in response to the overexpression of FOXL1 using qRT-PCR and found that FOXL1 over-expression induced pro-apoptotic gene TRAIL expression by about 2.5 fold in pancreatic cancer cell lines as compared to

controls ($P < 0.01$, Figure 3B). Consistent with the gene expression, the protein level of TRAIL was also increased about 2 fold in FOXL1 overexpressing cells.

Next, we investigated the mechanism of TRAIL induction following FOXL1 expression. ChIP-PCR assays showed the binding of FOXL1 protein to the TRAIL promoter ($P < 0.01$, Figure 3C). The promoter region (-1523 to +23, relative to the transcription start site) of TRAIL was then inserted into the pGL4 basic luciferase reporter vector (pGL4-TRAIL) as previously described (16). The luciferase activities of pGL4-TRAIL were significantly upregulated by 4.4-fold ($P < 0.01$) when it was co-transfected with pCMV-FOXL1 compared with pCMV-CTRL in Panc1 cells, and 5.7-fold in Miapaca2 cells ($P < 0.01$, Figure 3D). These findings indicate that FOXL1 induces the expression and promoter activity of TRAIL.

We further defined the role of TRAIL in FOXL1-induced apoptosis using an antibody directed against TRAIL in FOXL1 overexpressing cells. After transfection, Panc1 and MIApaca2 cells were treated with anti-TRAIL antibody (30 μ g/ml). Anti-TRAIL antibodies significantly blocked FOXL1-induced apoptosis (Figure 3E). Taken together, these results indicate that FOXL1 promotes apoptosis in pancreatic cancer, at least partly, through the induction of TRAIL expression.

FOXL1 inhibits migration and invasion ability of PDAC cells

To investigate the effect of FOXL1 on cancer cell migration and invasion, the monolayer scratch healing and Matrigel invasion assays were performed. Quantitative analyses demonstrated a significant reduction in wound closure in FOXL1-transfected cells as compared to control cells ($P < 0.01$, Figure 4A). In addition, high level of FOXL1 expression also significantly impaired the invasiveness of both Panc1 and MIApaca2 in Matrigel invasion assays using 10% FBS as a chemoattractant ($P < 0.01$, Figure 4B). In contrast, knock-down of FOXL1 promoted pancreatic cancer cell invasion ($P < 0.05$, supplementary Figure S3B).

FOXL1 binds to the promoter of ZEB1 and suppresses ZEB1 transcription

ZEB1 functions as an EMT-activator, promoting cancer cell invasion and aggressiveness (17). It has been reported that ZEB1 expression is higher in Panc1 and MIApaca2, pancreatic cancer cell lines with mesenchymal features, as compared with HPAF, Capan1, and Capan2 cell lines with epithelial features (18). We observed an inverse association between FOXL1 and ZEB1 expressions in pancreatic cancer cell lines (supplementary Figure S1A). Quantitative RT-PCR and western blot analyses showed that FOXL1 was higher in HPAF, Capan1, and Capan2 cell lines, and lower in Panc1 and MIApaca2 cells (Figure S1). We then tested the hypothesis that a higher level of FOXL1 suppresses ZEB1 expression. Quantitative RT-PCR and western blot analyses showed that overexpression of FOXL1 significantly inhibited ZEB1 expression in Panc1 and Miapaca2 cells (Figure 5A). In contrast, knock-down of FOXL1 increases the expression of ZEB1 ($P < 0.05$, supplementary Figure S1). To determine whether ZEB1 is involved in inhibitory effect of FOXL1 on cell invasion in pancreatic cancer, pancreatic cancer cell lines were transfected with si-FOXL1 alone or together with si-ZEB1. The stimulatory effect of FOXL1 knockdown on cell invasion was ablated by simultaneous siRNA mediated knockdown of ZEB1 (supplementary Figure S3B). These data indicated that the negative regulation of ZEB1 may contribute to the inhibitory effect of FOXL1 on invasion ability of pancreatic cancer cells.

Analysis of ZEB1 promoter to identify potential forkhead box binding sites using TRANSFAC program revealed 4 regions containing multiple potential FOXL1-binding sites at the upstream of transcription start site of ZEB1 (Figure 5B). To further investigate the

mechanism of FOXL1 mediated regulation of ZEB1, ChIP-PCR assays were performed to determine if a physical interaction exists between FOXL1 protein and the promoter region of ZEB1. We pulled down FOXL1-targeted DNA fragments and probed for 4 fragments representing different ZEB1 promoter regions by qRT-PCR (Figure 5C). The strongest association was detected around region-4 within the ZEB1 promoter ($P < 0.01$). We next tested whether this interaction affects ZEB1 transcription. The promoter region of ZEB1 harboring region-4 was inserted into the pGL4 basic reporter vector (pGL4-ZEB1). Luciferase activity was determined following co-transfection of pGL4-ZEB1 with pCMV-FOXL1 or pCMV control vector. As shown in Figure 5D, the luciferase activities of pGL4-ZEB1 were significantly decreased when it was co-transfected with pCMV-FOXL1 compared to pCMV-CTRL ($P < 0.01$, Figure 5D). These findings showed that FOXL1 bound to the promoter region of ZEB1 and suppressed transcription and promoter activity of ZEB1.

Discussion

FOXL1 was previously described as a critical transcriptional factor that regulates cell proliferation and development of epithelium in gastrointestinal tracts in mice (9). We performed OncoPrint database analyses on publicly available microarray datasets and found that FOXL1 expression is consistently decreased in multiple myeloma as compared to normal tissues, with a cut-off P value < 0.05 in microarray studies (19–21). One myeloma dataset also showed that FOXL1 is significantly higher in long survival (alive over a year) as compared with short survival group (dead within a year) (20). However, differential expression of FOXL1 between pancreatic tumors and non-tumors in available microarray datasets from OncoPrint are inconsistent (supplementary Figure S2). A lower FOXL1 expression was found in pancreatic tumors as compared with non-tumor pancreas tissues in two publicly available microarray datasets (22, 23). Interestingly, Ishikawa's data showed that FOXL1 level was significantly lower in pancreatic juice from pancreatic cancer patients than in healthy donors (24). In contrast, overexpression of FOXL1 in tumors was found in Pei's dataset (25) and no significant difference exists in FOXL1 expression between tumor and normal tissues in Grutzmann's dataset (26). Gene expression profile of Prasad's dataset showed a higher gene expression of FOXL1 in microdissected early PanIN lesions as compared to microdissected normal duct epithelium (27). In our study, IHC analysis which allows us to compare the FOXL1 expression in ductal cells demonstrated that low FOXL1 expression is correlated with metastasis and advanced pathological stage of pancreatic cancer (Figure 1). Moreover, our data showed for the first time that a higher FOXL1 expression is associated with better clinical outcome in resected PDAC cases. Functional studies revealed that restoration of FOXL1 in Panc1 and MIApaca2 pancreatic cancer cells significantly promoted apoptosis, inhibited cell proliferation, and suppressed cell invasion. Taken together, our findings support the inhibitory role of FOXL1 in pancreatic cancer.

Furthermore, we identified ZEB1 as a novel transcriptional target of FOXL1. ZEB1, encoded by the TCF8 gene, plays an important role in invasion and metastasis of human tumors (17). Enforced expression of ZEB in epithelial cells results in a rapid EMT associated with a breakdown of cell polarity, loss of cell–cell adhesion and induction of cell motility (28). Expression of ZEB1 promotes metastasis of tumor cells in a mouse xenograft model (29). Vice versa, knockdown of ZEB factors in cancer cells inhibit cell invasion (30). In this study, we showed that FOXL1 protein directly binds to ZEB1 promoter and suppresses the transcription and promoter activity of ZEB1 (Figure 5). Our data indicate that inhibition of ZEB1 expression by FOXL1 may contribute to the inhibitory effect of FOXL1 on invasive ability of pancreatic cancer cells.

Apoptosis plays a critical role in tumorigenesis. Several members of Fox family have been linked to the regulation of apoptosis in cancer (31). For example, FOXO proteins regulate

cell survival by modulating the expression of death receptor ligands (such as, FasL and TRAIL) which function in autocrine and paracrine manners (16, 32). In addition to the death receptor ligands, FOXO proteins have been shown to be involved in the transactivation of the Bcl-2 family, which has both pro- and anti-apoptotic members and plays a critical role in regulating cell survival (33, 34). In our study, the induction of apoptosis by FOXL1 appeared to be associated with upregulation of TRAIL expression.

TRAIL is a member of the tumor necrosis factor superfamily that is expressed in most human tissues (35, 36). The ligation of TRAIL with two receptors, called death receptor 4 (DR4, TRAIL-R1) and death receptor 5 (DR5, TRAIL-R2) (37–39), triggers apoptosis by recruiting the initiator caspase-8, which can directly activate downstream effector caspases, including caspase-3, caspase-6, and caspase-7(40). The potent death-inducing ability makes TRAIL an attractive candidate for cancer therapy (41). TRAIL has been reported to induce apoptosis in a wide spectrum of cancer cell lines including pancreatic cancer cell lines, with no or minimal toxicity on normal human cells (42–45). We found that enforced expression of FOXL1 resulted in an increased TRAIL expression in pancreatic cancer cells which eventually led to the elevated caspase-3 activity in these cells (Figure 3). There was no difference in TRAIL-R1 or R2 expression in FOXL1 overexpressing cells as compared to control cells. We also found a ~1.5 fold increase in Fas expression in these cells (supplementary Figure S4). However, several studies have shown that PDAC is resistant to Fas/CD95-mediated apoptosis, even though both Fas receptor and Fas ligand are frequently expressed in PDAC cells (46, 47). Thus, increased Fas expressions have limited impact on the induction of apoptosis by FOXL1, at least in pancreatic cancer.

In summary, our findings demonstrated for the first time that FOXL1 plays an inhibitory role in pancreatic cancer. Overexpression of FOXL1 promoted apoptosis, suppressed cellular growth and invasion in pancreatic cancer cells, at least partly through regulation of TRAIL and ZEB1 expression. These results are consistent with our finding that a higher FOXL1 expression is associated with better clinical outcome in PDAC patients. Therefore we propose that FOXL1 may function as a potential tumor suppressor and serve as a candidate predictor of outcomes in pancreatic cancer. Further studies are warranted to determine the molecular mechanism driving the loss of FOXL1 during pancreatic cancer progression and how the restoration of FOXL1 can be harnessed for therapeutic benefit.

Supplementary Material

Refer to Web version on PubMed Central for supplementary material.

Acknowledgments

Grant support: Intramural Research Program of the National Cancer Institute, Center for Cancer Research, NIH.

We would like to thank Drs. Stefan Ambs and Xin Wei Wang (National Cancer Institute) for helpful discussions. Handling of clinical samples and maintenance of tissue database by Ms. Elise Bowman, and histopathological evaluation by Dr. Matthias Gaida are highly appreciated.

References

1. Siegel R, Naishadham D, Jemal A. Cancer statistics, 2012. *CA Cancer J Clin.* 2012; 62:10–29. [PubMed: 22237781]
2. Hannenhalli S, Kaestner KH. The evolution of Fox genes and their role in development and disease. *Nat Rev Genet.* 2009; 10:233–40. [PubMed: 19274050]
3. Carter ME, Brunet A. FOXO transcription factors. *Curr Biol.* 2007; 17:R113–4. [PubMed: 17307039]

4. Paik JH, Kollipara R, Chu G, Ji H, Xiao Y, Ding Z, et al. FoxOs are lineage-restricted redundant tumor suppressors and regulate endothelial cell homeostasis. *Cell*. 2007; 128:309–23. [PubMed: 17254969]
5. Tothova Z, Kollipara R, Huntly BJ, Lee BH, Castrillon DH, Cullen DE, et al. FoxOs are critical mediators of hematopoietic stem cell resistance to physiologic oxidative stress. *Cell*. 2007; 128:325–39. [PubMed: 17254970]
6. Wang Z, Ahmad A, Li Y, Banerjee S, Kong D, Sarkar FH. Forkhead box M1 transcription factor: a novel target for cancer therapy. *Cancer Treat Rev*. 2009; 36:151–6. [PubMed: 20022709]
7. Xia JT, Wang H, Liang LJ, Peng BG, Wu ZF, Chen LZ, et al. Overexpression of FOXM1 Is Associated With Poor Prognosis and Clinicopathologic Stage of Pancreatic Ductal Adenocarcinoma. *Pancreas*. 2012; 41:629–35. [PubMed: 22249132]
8. Wang Z, Banerjee S, Kong D, Li Y, Sarkar FH. Down-regulation of Forkhead Box M1 transcription factor leads to the inhibition of invasion and angiogenesis of pancreatic cancer cells. *Cancer Res*. 2007; 67:8293–300. [PubMed: 17804744]
9. Kaestner KH, Silberg DG, Traber PG, Schutz G. The mesenchymal winged helix transcription factor Fkh6 is required for the control of gastrointestinal proliferation and differentiation. *Genes Dev*. 1997; 11:1583–95. [PubMed: 9203584]
10. Perreault N, Katz JP, Sackett SD, Kaestner KH. Foxl1 controls the Wnt/beta-catenin pathway by modulating the expression of proteoglycans in the gut. *J Biol Chem*. 2001; 276:43328–33. [PubMed: 11555641]
11. Perreault N, Sackett SD, Katz JP, Furth EE, Kaestner KH. Foxl1 is a mesenchymal Modifier of Min in carcinogenesis of stomach and colon. *Genes Dev*. 2005; 19:311–5. [PubMed: 15650110]
12. Moller E, Hornick JL, Magnusson L, Veerla S, Domanski HA, Mertens F. FUS-CREB3L2/L1-positive sarcomas show a specific gene expression profile with upregulation of CD24 and FOXL1. *Clin Cancer Res*. 2011; 17:2646–56. [PubMed: 21536545]
13. Aaltonen, LA.; Hamilton, SR. World Health Organization., International Agency for Research on Cancer. Pathology and genetics of tumours of the digestive system. Lyon, Oxford: IARC Press; Oxford University Press (distributor); 2000.
14. Glynn SA, Boersma BJ, Dorsey TH, Yi M, Yfantis HG, Ridnour LA, et al. Increased NOS2 predicts poor survival in estrogen receptor-negative breast cancer patients. *J Clin Invest*. 2010; 120:3843–54. [PubMed: 20978357]
15. Warner SL, Stephens BJ, Nwokenkwo S, Hostetter G, Sugeng A, Hidalgo M, et al. Validation of TPX2 as a potential therapeutic target in pancreatic cancer cells. *Clin Cancer Res*. 2009; 15:6519–28. [PubMed: 19861455]
16. Modur V, Nagarajan R, Evers BM, Milbrandt J. FOXO proteins regulate tumor necrosis factor-related apoptosis inducing ligand expression. Implications for PTEN mutation in prostate cancer. *J Biol Chem*. 2002; 277:47928–37. [PubMed: 12351634]
17. Aigner K, Dampier B, Descovich L, Mikula M, Sultan A, Schreiber M, et al. The transcription factor ZEB1 (deltaEF1) promotes tumour cell dedifferentiation by repressing master regulators of epithelial polarity. *Oncogene*. 2007; 26:6979–88. [PubMed: 17486063]
18. Wellner U, Schubert J, Burk UC, Schmalhofer O, Zhu F, Sonntag A, et al. The EMT-activator ZEB1 promotes tumorigenicity by repressing stemness-inhibiting microRNAs. *Nat Cell Biol*. 2009; 11:1487–95. [PubMed: 19935649]
19. Agnelli L, Mosca L, Fabris S, Lionetti M, Andronache A, Kwee I, et al. A SNP microarray and FISH-based procedure to detect allelic imbalances in multiple myeloma: an integrated genomics approach reveals a wide gene dosage effect. *Genes Chromosomes Cancer*. 2009; 48:603–14. [PubMed: 19396863]
20. Carrasco DR, Tonon G, Huang Y, Zhang Y, Sinha R, Feng B, et al. High-resolution genomic profiles define distinct clinico-pathogenetic subgroups of multiple myeloma patients. *Cancer Cell*. 2006; 9:313–25. [PubMed: 16616336]
21. Zhan F, Barlogie B, Arzoumanian V, Huang Y, Williams DR, Hollmig K, et al. Gene-expression signature of benign monoclonal gammopathy evident in multiple myeloma is linked to good prognosis. *Blood*. 2007; 109:1692–700. [PubMed: 17023574]

22. Badea L, Herlea V, Dima SO, Dumitrascu T, Popescu I. Combined gene expression analysis of whole-tissue and microdissected pancreatic ductal adenocarcinoma identifies genes specifically overexpressed in tumor epithelia. *Hepatogastroenterology*. 2008; 55:2016–27. [PubMed: 19260470]
23. Segara D, Biankin AV, Kench JG, Langusch CC, Dawson AC, Skalicky DA, et al. Expression of HOXB2, a retinoic acid signaling target in pancreatic cancer and pancreatic intraepithelial neoplasia. *Clin Cancer Res*. 2005; 11:3587–96. [PubMed: 15867264]
24. Ishikawa M, Yoshida K, Yamashita Y, Ota J, Takada S, Kisanuki H, et al. Experimental trial for diagnosis of pancreatic ductal carcinoma based on gene expression profiles of pancreatic ductal cells. *Cancer Sci*. 2005; 96:387–93. [PubMed: 16053509]
25. Pei H, Li L, Fridley BL, Jenkins GD, Kalari KR, Lingle W, et al. FKBP51 affects cancer cell response to chemotherapy by negatively regulating Akt. *Cancer Cell*. 2009; 16:259–66. [PubMed: 19732725]
26. Grutzmann R, Pilarsky C, Ammerpohl O, Luttgies J, Bohme A, Sipsos B, et al. Gene expression profiling of microdissected pancreatic ductal carcinomas using high-density DNA microarrays. *Neoplasia*. 2004; 6:611–22. [PubMed: 15548371]
27. Prasad NB, Biankin AV, Fukushima N, Maitra A, Dhara S, Elkahlon AG, et al. Gene expression profiles in pancreatic intraepithelial neoplasia reflect the effects of Hedgehog signaling on pancreatic ductal epithelial cells. *Cancer Res*. 2005; 65:1619–26. [PubMed: 15753353]
28. Browne G, Sayan AE, Tulchinsky E. ZEB proteins link cell motility with cell cycle control and cell survival in cancer. *Cell Cycle*. 2010; 9:886–91. [PubMed: 20160487]
29. Spaderna S, Schmalhofer O, Wahlbuhl M, Dimmler A, Bauer K, Sultan A, et al. The transcriptional repressor ZEB1 promotes metastasis and loss of cell polarity in cancer. *Cancer Res*. 2008; 68:537–44. [PubMed: 18199550]
30. Brabletz S, Brabletz T. The ZEB/miR-200 feedback loop--a motor of cellular plasticity in development and cancer? *EMBO Rep*. 2010; 11:670–7. [PubMed: 20706219]
31. Fu Z, Tindall DJ. FOXOs, cancer and regulation of apoptosis. *Oncogene*. 2008; 27:2312–9. [PubMed: 18391973]
32. Brunet A, Bonni A, Zigmond MJ, Lin MZ, Juo P, Hu LS, et al. Akt promotes cell survival by phosphorylating and inhibiting a Forkhead transcription factor. *Cell*. 1999; 96:857–68. [PubMed: 10102273]
33. Sunters A, Fernandez de Mattos S, Stahl M, Brosens JJ, Zoumpoulidou G, Saunders CA, et al. FoxO3a transcriptional regulation of Bim controls apoptosis in paclitaxel-treated breast cancer cell lines. *J Biol Chem*. 2003; 278:49795–805. [PubMed: 14527951]
34. Dijkers PF, Medema RH, Lammers JW, Koenderman L, Coffey PJ. Expression of the pro-apoptotic Bcl-2 family member Bim is regulated by the forkhead transcription factor FKHR-L1. *Curr Biol*. 2000; 10:1201–4. [PubMed: 11050388]
35. Wiley SR, Schooley K, Smolak PJ, Din WS, Huang CP, Nicholl JK, et al. Identification and characterization of a new member of the TNF family that induces apoptosis. *Immunity*. 1995; 3:673–82. [PubMed: 8777113]
36. Pitti RM, Marsters SA, Ruppert S, Donahue CJ, Moore A, Ashkenazi A. Induction of apoptosis by Apo-2 ligand, a new member of the tumor necrosis factor cytokine family. *J Biol Chem*. 1996; 271:12687–90. [PubMed: 8663110]
37. Pan G, O'Rourke K, Chinnaiyan AM, Gentz R, Ebner R, Ni J, et al. The receptor for the cytotoxic ligand TRAIL. *Science*. 1997; 276:111–3. [PubMed: 9082980]
38. Pan G, Ni J, Wei YF, Yu G, Gentz R, Dixit VM. An antagonist decoy receptor and a death domain-containing receptor for TRAIL. *Science*. 1997; 277:815–8. [PubMed: 9242610]
39. MacFarlane M, Ahmad M, Srinivasula SM, Fernandes-Alnemri T, Cohen GM, Alnemri ES. Identification and molecular cloning of two novel receptors for the cytotoxic ligand TRAIL. *J Biol Chem*. 1997; 272:25417–20. [PubMed: 9325248]
40. Ashkenazi A. Targeting death and decoy receptors of the tumour-necrosis factor superfamily. *Nat Rev Cancer*. 2002; 2:420–30. [PubMed: 12189384]
41. LeBlanc HN, Ashkenazi A. Apo2L/TRAIL and its death and decoy receptors. *Cell Death Differ*. 2003; 10:66–75. [PubMed: 12655296]

42. Leverkus M, Neumann M, Mengling T, Rauch CT, Brocker EB, Krammer PH, et al. Regulation of tumor necrosis factor-related apoptosis-inducing ligand sensitivity in primary and transformed human keratinocytes. *Cancer Res.* 2000; 60:553–9. [PubMed: 10676636]
43. Gazitt Y. TRAIL is a potent inducer of apoptosis in myeloma cells derived from multiple myeloma patients and is not cytotoxic to hematopoietic stem cells. *Leukemia.* 1999; 13:1817–24. [PubMed: 10557057]
44. Satoh K, Kaneko K, Hirota M, Masamune A, Satoh A, Shimosegawa T. Tumor necrosis factor-related apoptosis-inducing ligand and its receptor expression and the pathway of apoptosis in human pancreatic cancer. *Pancreas.* 2001; 23:251–8. [PubMed: 11590320]
45. Kim K, Fisher MJ, Xu SQ, el-Deiry WS. Molecular determinants of response to TRAIL in killing of normal and cancer cells. *Clin Cancer Res.* 2000; 6:335–46. [PubMed: 10690508]
46. Satoh K, Shimosegawa T, Masamune A, Hirota M, Koizumi M, Toyota T. Fas ligand is frequently expressed in human pancreatic duct cell carcinoma. *Pancreas.* 1999; 19:339–45. [PubMed: 10547193]
47. Ungefroren H, Voss M, Jansen M, Roeder C, Henne-Bruns D, Kremer B, et al. Human pancreatic adenocarcinomas express Fas and Fas ligand yet are resistant to Fas-mediated apoptosis. *Cancer Res.* 1998; 58:1741–9. [PubMed: 9563493]

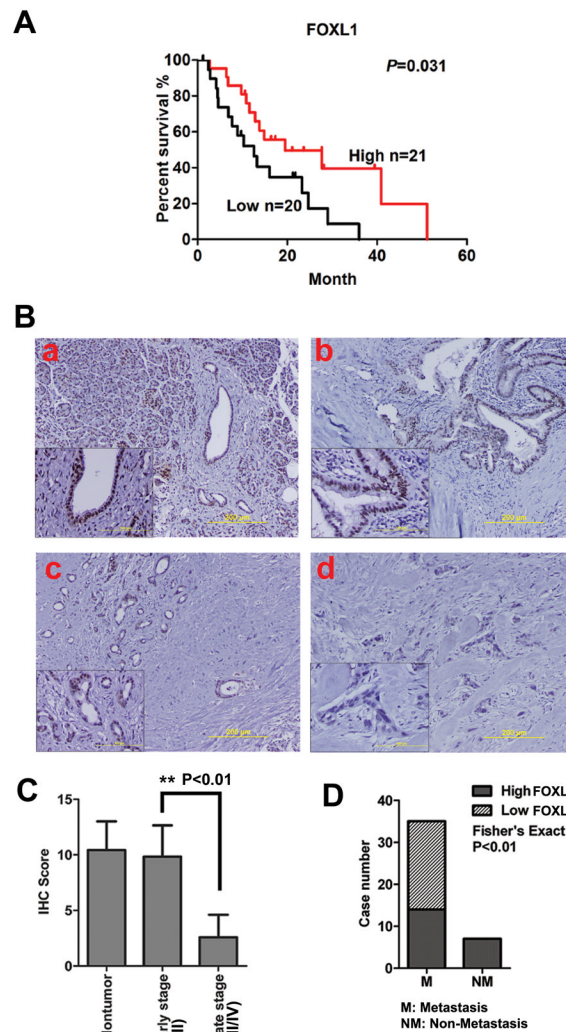


Figure 1. Higher FOXL1 gene expression is associated with better clinical outcome in PDAC (A) Kaplan Meier analysis based on FOXL1 expression levels in PDAC. FOXL1 gene expression values were determined by qRT-PCR and dichotomized into high and low groups using median value. Survival profiles were compared using the log-rank test. (B) Representative images of immunohistochemical staining of FOXL1 in normal ductal cells (a), PanIN lesions (b), moderately differentiated tumors (c) and poorly differentiated tumors (d). Original magnification, 200X. Scale bar, 200 μ M. (C) FOXL1 immunostaining is weaker in late stage (III/IV) as compared with early stage (I/II) tumors (*t*-test, $P < 0.01$). The intensity was assigned a score of 0–3, representing negative, weak, moderate or strong expression, whereas, prevalence was assigned a score of 0–4 representing <10%, 10–30%, 30–50%, 50–80% and >80% cells showing FOXL1 expression. The overall quantitation of IHC score was then achieved by multiplying the intensity and prevalence score as previously described. (D) A lower expression of FOXL1 is associated with cases showing lymph node and distant metastases. Tumors were defined as high FOXL1-staining if their total IHC score was greater than 6 and low staining if their score was less than or equal to 6. *P*-value for Fisher's exact test was indicated.

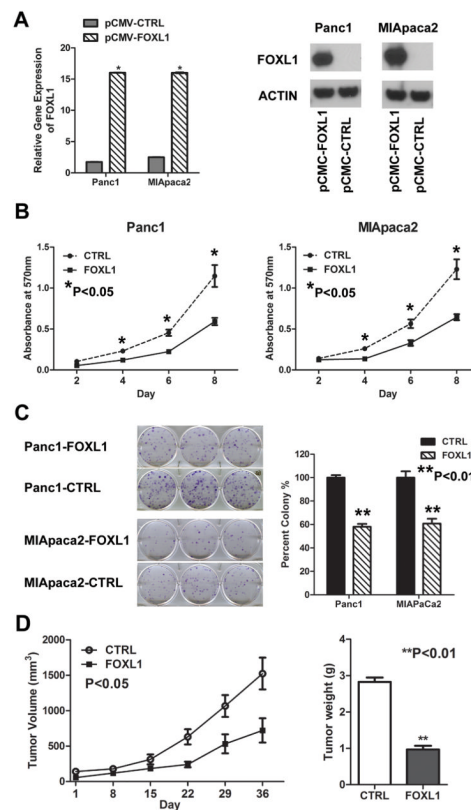


Figure 2. FOXL1 inhibits pancreatic tumor growth

(A) Increased expression of FOXL1 in transfected pancreatic cancer cells were demonstrated by qRT-PCR and western blot analysis. (B) There were significant decreases in cell growth of FOXL1 overexpressing cells as compared with control cells. (C) FOXL1 overexpressing cells exhibited reduced colony formation as compared with control cells. Data are presented as means \pm S.D. from 3 independent experiments. ** *t*-test $P < 0.01$. (D) Subcutaneous implantation of FOXL1-overexpressing Panc1 cells in nude mice, showed a significant decrease in tumor growth as compared to control cells.

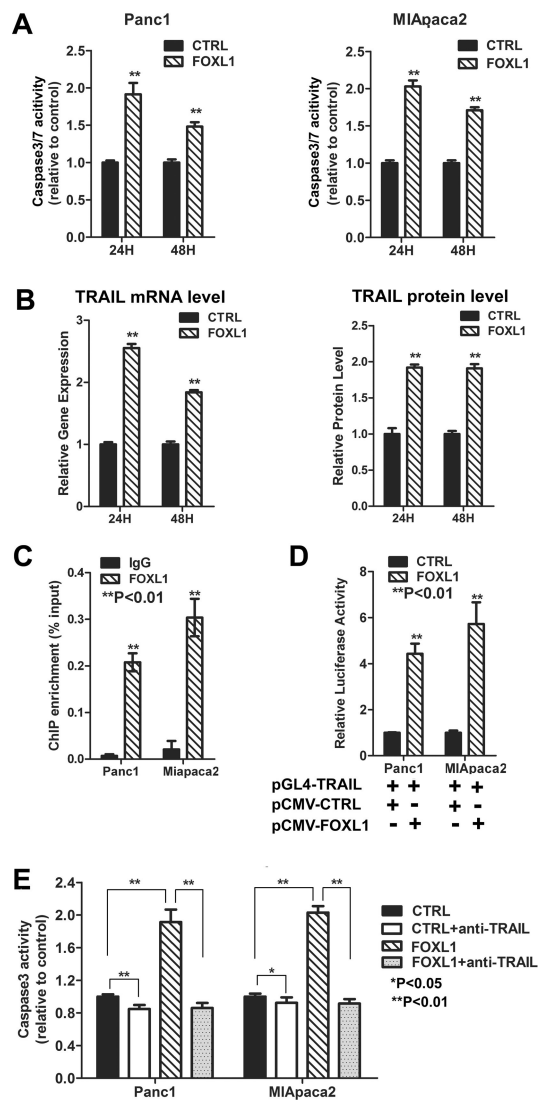


Figure 3. FOXL1 induces TRAIL expression and promotes apoptosis

(A) Overexpression of FOXL1 led to a significant increase in caspase-3/7 activity in Panc1 and MIApaca2 cells ($P < 0.01$). Relative Caspase3/7 activity represents the effect of FOXL1 overexpression on apoptosis compared to control cells at 24h and 48h post-transfection. (B) FOXL1-overexpression upregulated TRAIL expression. Real-time PCR was performed to determine TRAIL mRNA levels. TRAIL protein level in cell lysates was measured using ELISA kit (R&D Systems) according to the manufacturer's instructions. (C) ChIP-PCR assay showed the binding of FOXL1 protein to the TRAIL promoter. ChIP assay was performed in Panc1 and MIApaca2 cells, followed by qRT-PCR using a primer pair for TRAIL promoter. Lysates were immunoprecipitated with control mouse IgG and anti-GFP antibody for GFP-tagged FOXL1. RT-PCR values were normalized to the total amount of DNA added to the reaction (input). Data are presented as percent input. (D) Luciferase reporter assays showed the stimulatory effect of FOXL1 on TRAIL transcription in Panc1 and MIApaca2 cells. The pGL4-TRAIL vector was cotransfected with FOXL1 expression vector pCMV-FOXL1 or empty vector pCMV-CTRL. Renilla luciferase transfection (pRL-TK) was also included in each assay for normalization in Dual-Luciferase Reporter Assay System (Promega). Each transfection was performed in triplicates. ** t -test $P < 0.01$. (E)

Anti-TRAIL antibodies blocked FOXL1-induced apoptosis. Data represent means \pm S.D. from 3 independent experiments. ** *t*-test $P < 0.01$.

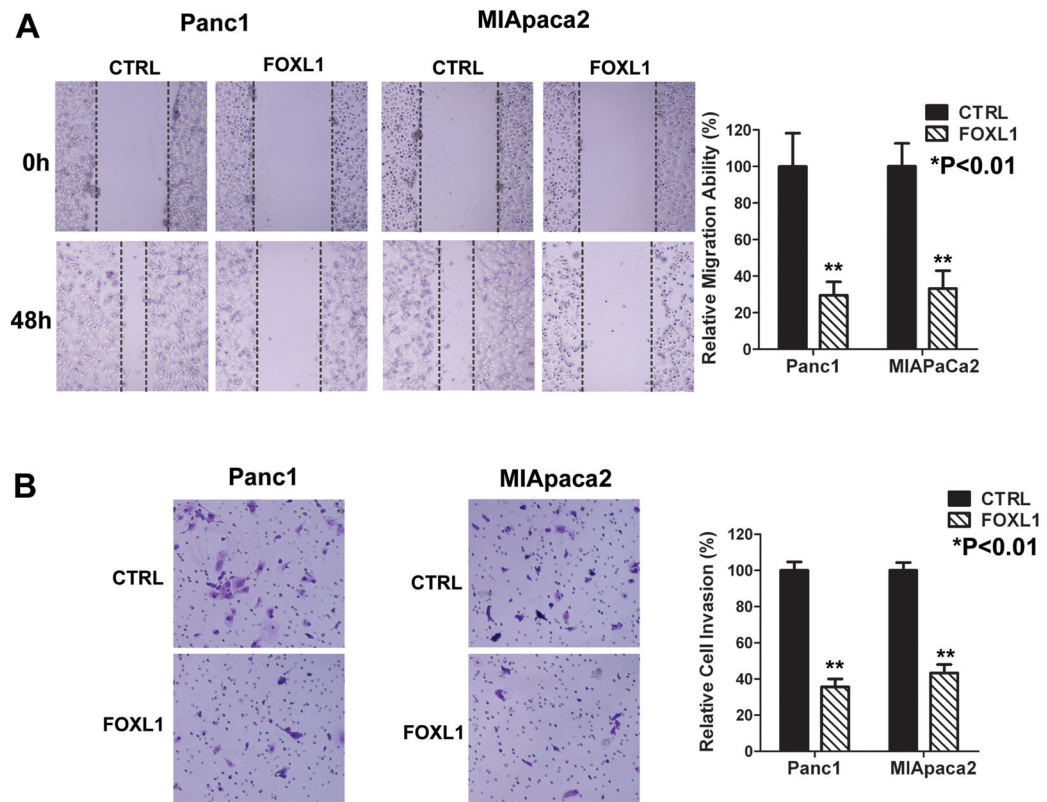


Figure 4. FOXL1 inhibits cell migration and invasion of pancreatic cancer cells

(A) Cell migration was assessed using scratch-healing assays. Confluent monolayer of Panc1 and Miapaca2 cells were scratched and healing was monitored by taking photographs at the indicated time points. (B) Cell invasion was determined in Panc1 and MIapaca2 cells using Biocoat matrigel invasion assay. The invaded cells were counted under a microscope. Data represent means \pm S.D. from 3 independent experiments. ** t -test $P < 0.01$.

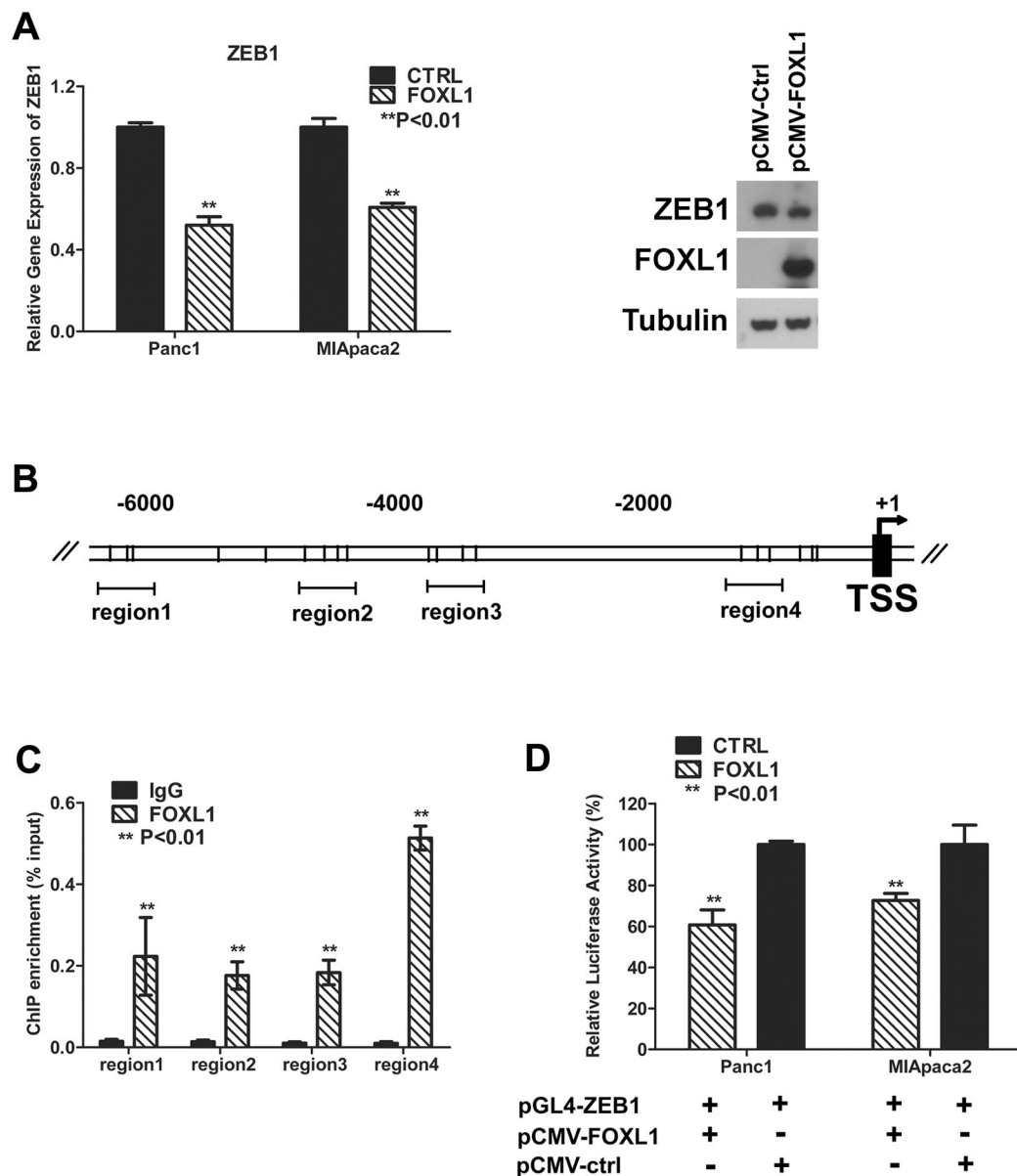


Figure 5. FOXL1 suppresses expression and promoter activity of ZEB1

(A) Overexpression of FOXL1 results in a decrease in ZEB1 expression as analyzed by qRT-PCR and western blotting. (B) Schematic representation of 5' upstream of transcriptional start site (TSS) of the *ZEB1* gene. Predicted forkhead box binding sites with good match were marked (Matrix similarity>0.9). (C) ChIP assay was performed in Panc1 cells, followed by qRT-PCR using primer pairs spanning 4 regions in *ZEB1* promoter. Lysates were immunoprecipitated with control mouse IgG and anti-GFP antibody for GFP-tagged FOXL1. Quantitative RT-PCR values were normalized to the total amount of DNA added to the reaction (input). Data are presented as percent input. (D) Luciferase reporter assays showed the inhibitory effect of FOXL1 on *ZEB1* transcription in Panc1 and MIApaca2 cells. The pGL4-ZEB1 vector was cotransfected with FOXL1 expression vector pCMV-FOXL1 or empty vector pCMV-ctrl. Renilla luciferase transfection (pRL-TK) was

also included in each assay for normalization in Dual-Luciferase Reporter Assay System (Promega). Each transfection was performed in triplicates. ** *t*-test $P < 0.01$.

Table 1

Cox regression analysis of FOXL1 expression with cancer-specific mortality in pancreatic cancer.

Variables (comparison/referent)	Univariate analysis		Multivariate analysis ^I	
	HR (95% CI)	<i>P</i>	HR (95% CI)	<i>P</i>
FOXL1(high/low)	0.44 (0.20–0.95)	0.036	0.41 (0.19–0.89)	0.024
Grading (G3&4/1&2)	2.77 (1.12–6.87)	0.027	2.93 (1.20–7.15)	0.018
Tumor stage (III-IV/I-II)	2.51 (0.76–8.69)	0.130		
Resection Margin (R1/R0)	1.62 (0.75–3.51)	0.220		

^IMultivariate analysis used stepwise addition and removal of clinical covariates found to be associated with survival in Univariate model and final models include only those covariates that were significantly associated with survival ($P < 0.05$).